

Burn-Rate Measurement of Methane-Air Mixture in a Spherical Vessel by a Diode-Laser Absorption Spectrometry

Ryuji Koga, Megumi Kosaka, Hiroya Sano*, Yoshisuke Hamamoto, and Eiji Tomita
The School of Engineering, Okayama University, Tsushima, Okayama 700
*Faculty of Engineering, Fukuyama University

ABSTRACT

Non-contacting and temporally continuous measurement was made for radius of spherical flame front on the progress of a single combustion. Abundance of unburned methane at a time instant was determined from an absorption spectrum obtained with using a chirping diode laser beam passing through the spherical vessel. The spectral scanning solved the problem of pressure-broadening which arises as the combustion progresses. Pressure was recorded simultaneously to exploit the adiabatic hypothesis. Stoichiometric methane-air mixture was filled in the vessel of 100 mm diameter with initial pressures ranging from 50 kPa to 200 kPa.

Experimental results are compared with those calculated only from the pressure with using a theory of Lewis and von-Elbe as well as those obtained with ion probes.

Results of three methods agree well when the initial pressure is low but do not at high pressure. This method has the advantage of the accuracy at the initial stage.

INTRODUCTION

The laminar combustion properties of fuel-air mixture at high temperature and pressure are of fundamental importance for modeling the turbulent combustion process in an internal combustion engine cylinder[1]. The spherical constant-volume technique has been considered one of the most suitable for investigating fundamental properties of laminar flame[2,3]. Measurement of flame-front positions is the fundamental requirement and has been done with ion probes which may introduce an undesirable disturbance to the flame.

It is generally recognized that optical methods are profitable for flame diagnosis because the least disturbance is expected. Flame positions have been detected with the diffraction of He-Ne laser beams[3,4,5], where flame fronts should traverse beams and a few data is obtained during a single combustion. Another beam arrangements in which the beam is perpendicular to the flame front is desirable for a continuous tracking.

The absorption method instead of the diffraction is appreciated for the advantage of specificity to a gas species and its higher sensitivity in comparison with a Raman scattering method. An absorption spectrum of a flammable gas is suffered from the pressure broadening at a combusting condition and a

single frequency laser light is useless to know abundance of the gas of interest. A tunable lead-salt diode laser provides a scheme to solve this problem.

A temporal evolution of the mass fraction burned is of concern in this paper. This value has been obtained by only a measured pressure through a thermodynamical treatments. The results gives, however, a poor accuracy at the initial stage where the pressure is still keeping its initial value though this stage is significant to know a flame speed under a constant pressure.

A new method proposed here gives a more close information especially in the initial stage just after the ignition and the flame radius can be measured continuously combining a pressure recorded simultaneously. Both the attenuation for the infrared laser beam and the pressure are measured without contacting the flame.

A lead-tin-terullide(PbSnTe) tunable diode laser (Pb-TDL) is featured with a continuous and quick tunability in the mid-infrared domain where most of gases has their absorption lines[6]. A quick and repeated spectral scanning over an absorption line makes it possible to know the abundance of gas left unburned though suffered from a collision broadening of the spectral profiles due to the increasing pressure.

A part of the authors have developed atmospheric gas monitors which achieve simultaneously portable, sensitive, non-sampling and real-time measurement capabilities[7]. A technique to drive a Pb-TDL by a pulsed current controlling its chirping characteristics has been developed there and is also applied to this study.

Pb-SALT DIODE LASERS

Tunability

A Pb-salt tunable diode laser (Pb-TDL) has its emission spectrum in the mid-infrared domain where many of gas of light molecular weight have their vibrational-rotational absorption lines. This laser is characterized by its continuous tunability through the junction temperature and by high spectral purity as well as by other features common with popular GaAs based lasers for communication use.

An example of the emission frequency as a function of the heat-sink temperature is given in Fig.1a. As the junction temperature rises, a refractive index of the material around the junction decreases and the emission wavelength too. The lower the temperature, the higher gain is attained

and longitudinally multimodal operation takes place, which is seen around 20K and 35K.

For a temperature higher than 80K, lasing is not achieved and a cryogenic cooler or a liquid nitrogen Dewar vessel is required. The junction temperature can be finely controlled by the Joule heating of the driving current through the junction. There shown is also a dependence of the lasing frequency on the driving current where the heat-sink temperature is kept at the liquid nitrogen temperature in Fig.1b. As the current increases, a mode hop takes place and multimode operation begins at the higher current region.

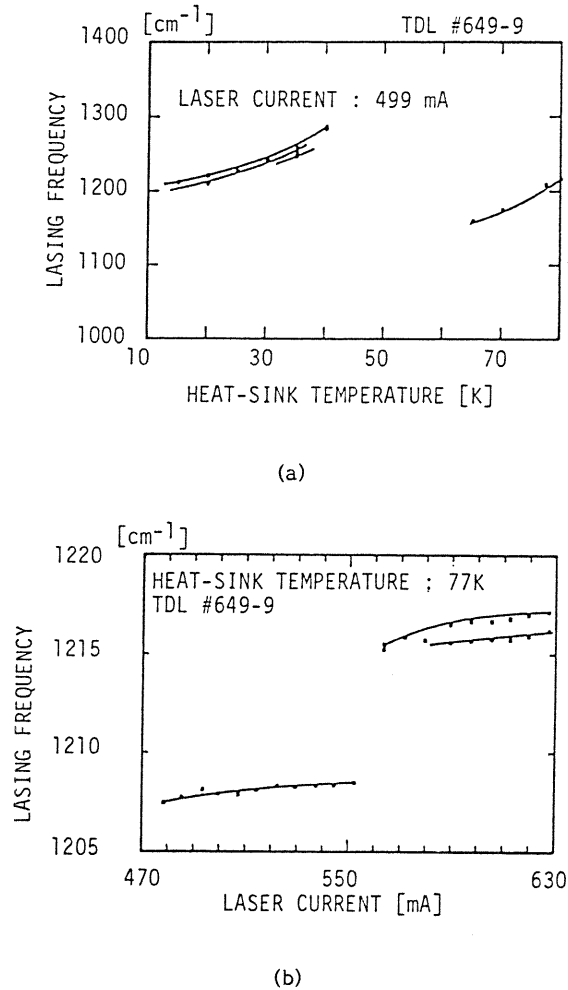


Fig.1 Tuning curves of the lasing frequency as a function of the heat-sink temperature, (a), and of the diode current, (b).

Temporal Response of Lasing Frequency

The junction temperature is subject to its thermal dynamics characterized by thermal capacity and thermal conductance between the junction and the heatsink. The timeconstant ranges around 10 micro-seconds so far as the authors have measured [8]. The lasing frequency chirps according to this time constant when a step current is applied as Fig.2. The frequency chirp was monitored with a Ge-etalon of 5 mm thick put across the collimated beam. One cycle of the undulation in the detector

output corresponds to a frequency chirp of 0.25 cm⁻¹ width. Total excursion of the chirp extends as the amplitude of the applied current, though is it still limited up to 2 cm⁻¹ for fear of thermal damage of the element.

The temporal response of the chirp is not linear for a stepwise current profile, which is inconvenient for a spectrometric purpose where correct line profiles are to be measured. A discrete-transistor based circuit was developed to control the current profile so that the chirping be linear in time within the period of 12 microseconds. A result is shown in Fig.3 where the linear chirping is achieved retaining the power profile in the detector at about a constant level.

ANALYSIS

As shown in Fig.4, stoichiometric methane-air mixture is contained with pressure p in a spherical vessel of radius a , and is ignited at the center at $t=0$. Let the flame be enough thin, the flame front expand in a concentric configuration, and the convective rise be negligible.

The laser beam passes through the sphere center with incident power W_I being attenuated down to the transmitted power W_T at the exit. The optical thickness τ is then written as

$$\tau(\nu) = \ln \frac{W_I}{W_T} = \tau_0 + 2(a-r_b)n_s \quad (1)$$

where ν is the laser frequency, r_b is the flame radius, and n is the molecular density of methane in the unburned region. Methane has its specific absorption coefficient s which is a function of ν and pressure p having a Lorentzian profile

$$s(\nu, p) = \frac{S}{\pi} \frac{\alpha^2}{(\nu - \nu_0)^2 + \alpha^2}, \quad (2)$$

where S is called as the line intensity and ν_0 is the line center. The parameter α stands for the half width at half maximum, and is further calculated [9] as

$$\alpha = \alpha_i (p/p_i) (\theta_i/\theta_u)^{1/2} \quad (3)$$

where θ stands for temperatures with suffix i for the initial and u for the unburned.

If laser light of single frequency is employed, no significant result is obtained even if the frequency hits the line center because it is still suffered from unknown τ_0 and the varying α according to the progress of the combustion.

Let us integrate s of eq.(2) with respect to ν to have a relation

$$S = \int_0^{\infty} s(\nu) d\nu. \quad (4)$$

It should be noted that S is independent of α . From this equation, the abundance $2(a-r_b)n$ of the unburned methane is calculated by measuring the spectral profile of τ repeatedly during the combustion. The parameter α is also a function of temperature. This effect can be neglected so far as

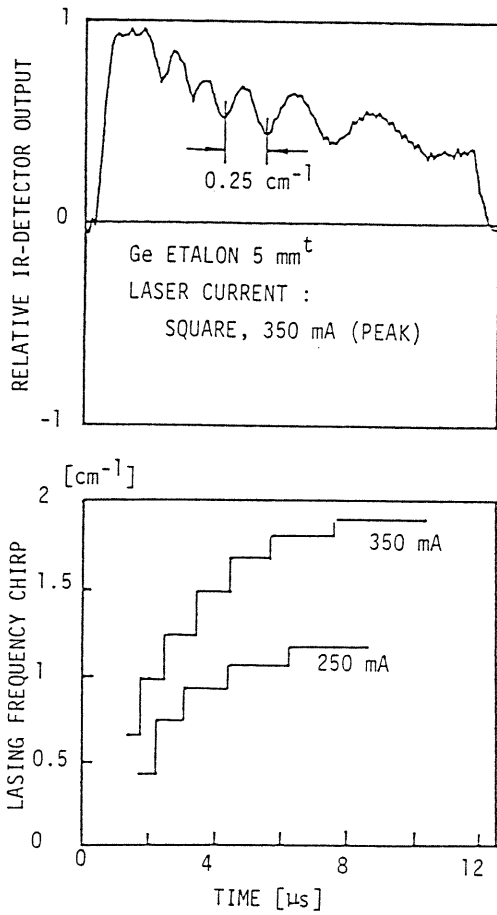


Fig.2 A chirping characteristics of a PbSnTe tunable diode laser.

the adiabatic change is concerned and the temperature rise is limited to 500K[9]. Thus an apparent absorption line intensity I is calculated as

$$I = \int_0^{\infty} \tau(\nu) d\nu = 2(a-r_b)nS. \quad (5)$$

Let normalize I , r_b and p as

$$\tilde{I} = I/I_i \quad (6)$$

$$\tilde{r} = r_b/a \quad (7)$$

and

$$\tilde{p} = p/p_i \quad (8)$$

Assuming the adiabatic compression of unburned gas and the homogeneous pressure distribution in the vessel, a relation

$$\tilde{I} = (1 - \tilde{r}) \tilde{p}^\lambda \quad (9)$$

or

$$\tilde{r}_{opt} = 1 - \tilde{I} / \tilde{p}^\lambda \quad (10)$$

is obtained, where a parameter λ is employed instead of κ for the sake of short expression.

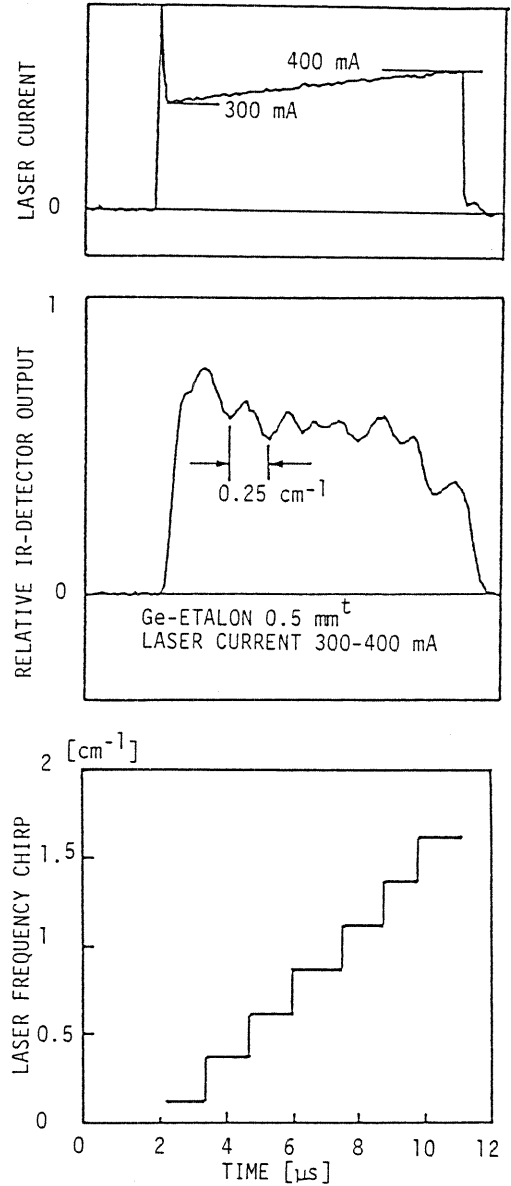


Fig.3 The chirping can be linearized with a controlled driving current for the diode laser.

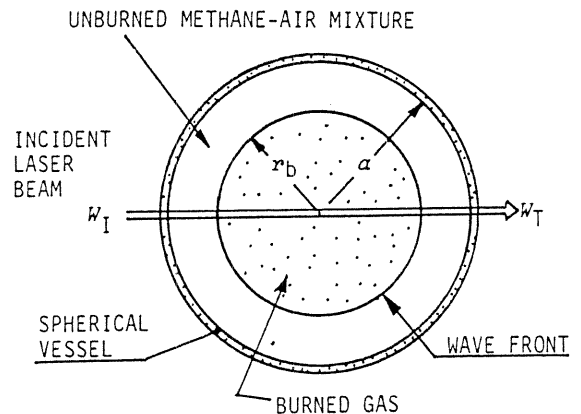


Fig.4 Geometry of the flame.

The mass fraction burned determined from both optical and pressure is written as

$$x_{opt} = 1 - \tilde{p}^\lambda (1 - \tilde{x}_{opt}^3). \quad (11)$$

The suffix "opt" is added since this x is known from the normalized apparent line intensity \tilde{I} in addition to the pressure \tilde{p} . Thus the x_{opt} can be known without contacting the flame.

Another estimate of x is already given by Lewis and von Elbe[10] as

$$x_p = \frac{p - p_i}{p_e - p_i}, \quad (12)$$

Where the suffix p stands for "pressure only" and p_e , the pressure at the final stage, when the flame-front arrives at the vessel wall.

A difference between x_p and x_{opt} is also found in that x_{opt} is a rather local value only integrated on the beam line, whereas x_p , a value integrated over the whole volume of the sphere. Equation (12) includes, however, some approximation in its derivation, and a comparison between x_p and x_{opt} is interesting. In this context, a radius of flame front is also derived from only the pressure, \tilde{p} , as

$$\tilde{r} = \{1 - \tilde{p}^\lambda (1 - x_p)\}^{-1/3}. \quad (13)$$

A rough relation between \tilde{x} and \tilde{I} is estimated from eqs.(11) and (12), and is shown in Fig.5, where \tilde{I} changes very rapidly when \tilde{x} is very small which corresponds to the initial stage. As will be shown later \tilde{I} changes linearly as time and is easier to measure than the small pressure rise at this stage. Thus more precise measurement on x is possible by eq.(11) than by eq.(12).

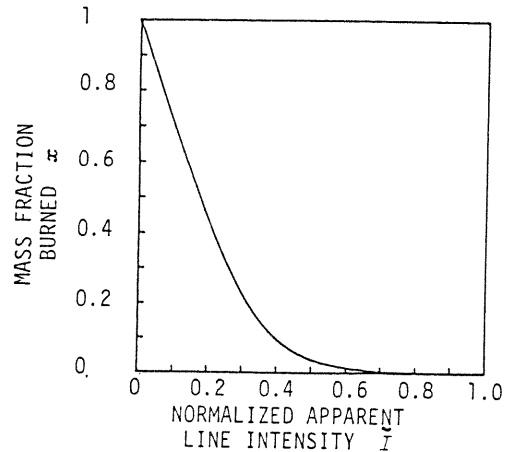


Fig.5 A general relation between the mass fraction burned and the apparent line intensity.

EXPERIMENTS

Set-Up

A schematic diagram is shown in Fig.6. A diverging emission from the lead-salt tunable diode laser (Pb-TDL) is collimated with an off-axis parabolic mirror (OAM) and is steered by two plane mirrors, M1 and M2, to pierce the spherical vessel B of inner radius $a=100$ mm at its center. The vessel is equipped with two germanium windows of 5 mm thickness and 8 mm diameter. Both sides of each window are uncoated and shaped in a wedge of 30° from parallel in order to avoid an etalon fringe.

For the ignition, a couple of needle electrodes are opposing at the center. One of them is grounded to the vessel and another is driven by an

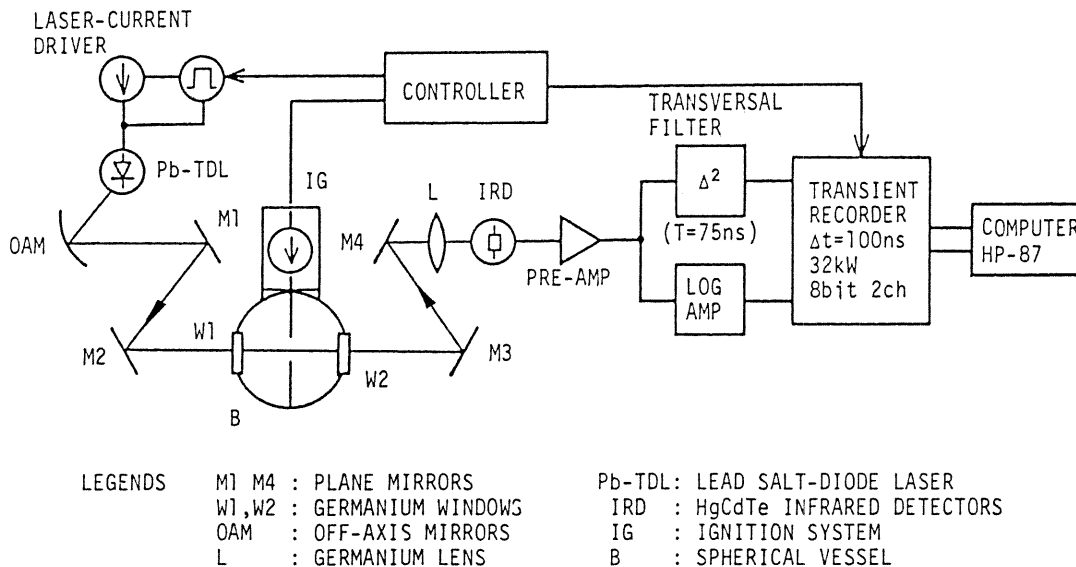


Fig.6 Schematic diagram of the experimental setup.

ignition-current driver which is designed so that the least electromagnetic impulse should be radiated to the environment where electronic measuring equipments are located. A CDI ignition circuit is installed in a closed metal cylinder and the electric energy is transferred to the gap in a transverse electromagnetic (TEM) mode.

The exit beam is steered again by mirrors M3 and M4, and focused by a Ge lens, L, onto an infrared detector (IRD) which is a liquid-nitrogen cooled PC-type HgCdTe device with its bandwidth extended to 10MHz at the sacrifice of the detectivity, D^* .

The IRD output is treated in twofold legs. One goes through a log-amplifier to extend the dynamic range and to have a correct optical thickness τ . Another leg has a transversal filter that produces a difference of second order with a unit delay time $T=75$ ns using a delay-line unit (Sony-Tektroniks 7M11) made as an oscilloscope plug-in unit. Second difference signal has a "band-pass" capability that can eliminate the background level shift and smooth variation in the temporal profile of the laser power. Both results are converted by a fast 8bit AD converters and are recorded in digital form.

The digital storage and control system was designed and build by the authors employing CMOS static RAMs having 32Kx2 words capacity in total.

The laser current drivers generates a current pulse of 10 microseconds pulse-width and its profile is controlled so that the TDL chirping be linear in time retaining the power level constant. In addition to the pulsed current, weak DC current is superimposed to control the junction temperature for the chirping spectral range hit a methane line at its center.

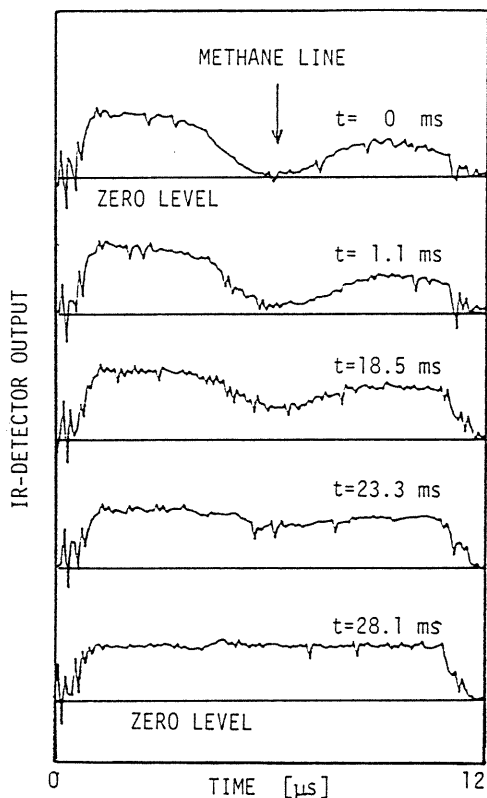


Fig.7 Example of recorded spectra during a single combustion.

Results

An example of a spectrum transient during a single combustion is shown in Fig.7. The absorption line located in the center is clearly recognized at the first stage of the combustion where pressure is still low and the line width is narrow. It grows wider and become weaker as the combustion progresses. At the last stage, the line profile can scarcely be recognized since the half width extends wider than the spectral range that the diode laser sweep.

Each spectrum is composed of 128 data items of 8-bits. During a single combustion, 256 spectra are recorded. The "alignment" of a line position onto the center of the scanning range requires a tuning of heat-sink temperature as well as of heat-up current avoiding a longitudinal mode-hop amid the spectral range. This result is cited for a clear illustration of the spectral profile that is involved in this experiment. Actually a diode element shown here ended its life and another element which is mounted on a Dewar vessel to keep the liquid nitrogen and it was unfortunately impossible to separate the available methane line and a mode hop over enough spectral separation.

Figures 8,9 and 10 are records of the pressure p obtained with a strain gauge, and of the normalized apparent line intensity \bar{I} for the initial pressures of 50 kPa, 100 kPa and 200 kPa, respectively. At just the initial stage, records are still suffered from the induction noise from the ignition system in spite of the carefully prepared architectures. The effect of non-spherical flame front profile is also recognized at this stage, though not proven yet.

For the lower initial pressure, the absorption line profile is narrower and the tracking for \bar{I} was more successful throughout the combustion than other cases of higher initial pressures. For the 50kPa case the value \bar{I} was calculated by employing the adjoint spectrum method [11] that was developed by the authors in the past, involving the whole spectral data. This algorithm is effective for the period when the pressure rise is small and the line profile is not broaden.

In the last stage where the pressure has risen, the line broadening prohibits an accurate calculation of \bar{I} in any methods. A possible error takes place towards the decrease of \bar{I} value from the truth, which is recognized in the \bar{I} trace in Fig.8 after about 20 milliseconds: the line obviously goes lower than is expected from the line extrapolated from values in the initial and medium stages.

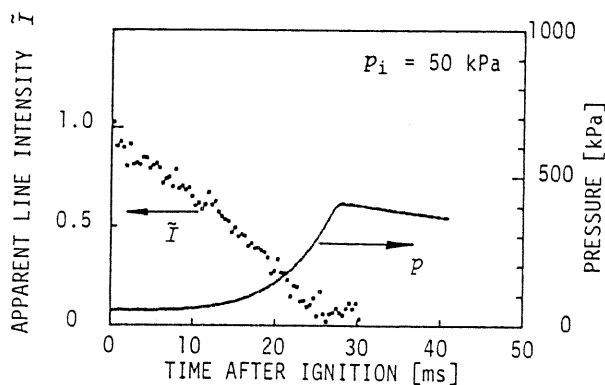


Fig.8 Progress of pressure and the line intensity calculated from the recorded spectra, both of a single combustion. The initial pressure was taken as $P_i=50$ kPa.

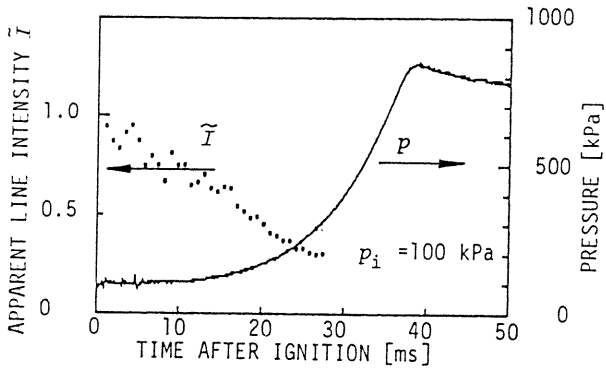


Fig.9 Progress of pressure p and the line intensity \tilde{I} calculated from the recorded spectra, both of a single combustion. The initial pressure was taken as $p_i = 100$ kPa.

Progress of a flame-front radius were calculated from these data with using eqs.(10) and (13). Experiments with ion probes were also made to know reference information. Results are shown in Fig.11 and 12, for $p_i = 50$ kPa and 100 kPa, respectively. For $p_i = 50$ kPa case in Fig.11, three results agree fairly well except at the just initial stage when the flame profile is considered to be different from the supposed sphere.

The optical method gives a non-zero radius at the initial stage. The probe beam runs through the center perpendicular to the ignition electrodes which may produce an in-line discharge pass which induces a disc-like flame-front profile for which the beam

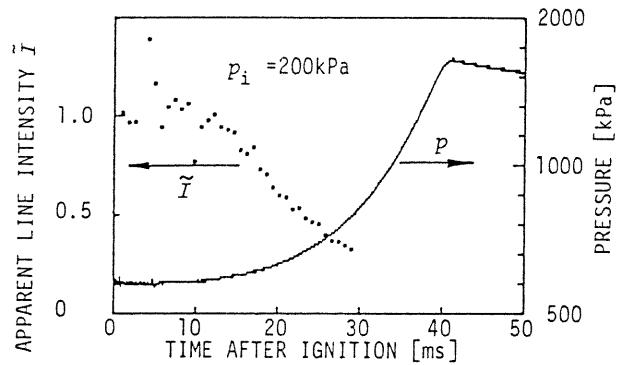


Fig.10 Progress of pressure p and the line intensity \tilde{I} calculated from the recorded spectra, both of a single combustion. The initial pressure was taken as $p_i = 200$ kPa.

passes along the line of upsides. A result determined after the Lewis-vonElbe (LvE) model is heavily disturbed at the initial stage beyond the range that a fitting with a 4th order polynomial track. A spectral profile is shown in the inset of Fig.11 showing the overlap of the methane spectrum and a modehop of TDL, which limited the accuracy of this series of experiments.

The coincidence between results with these three methods becomes, however, slightly poor in the higher initial pressure case, $p_i = 100$ kPa, as shown in Fig.12. The same treatment was done for the $p_i = 200$ kPa case but a results was too divergent to give a significant conclusion.

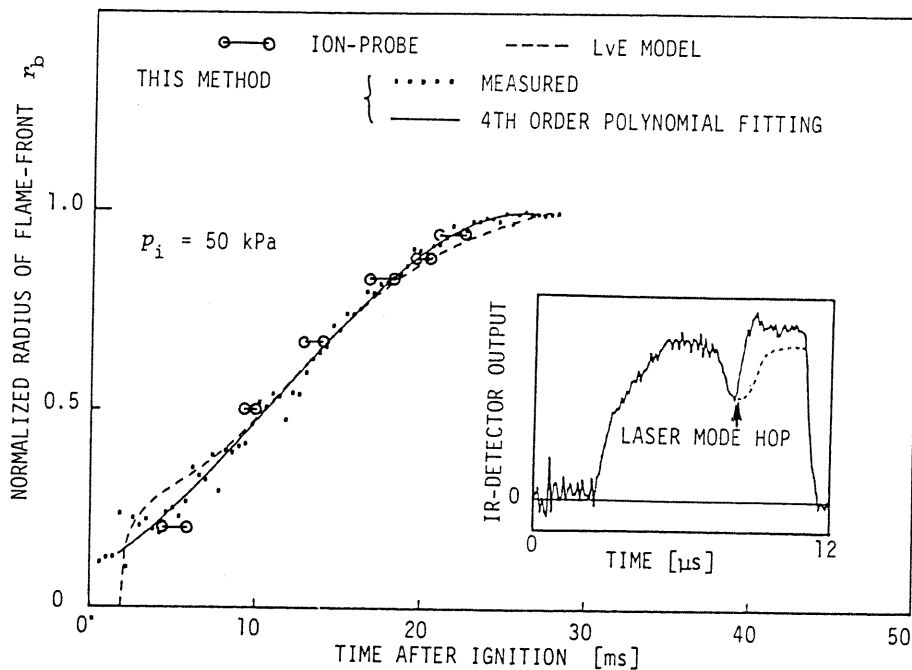


Fig.11 Progress of flame-front radii determined by three methods, ion probes, Lewis-vonElbe method from pressure only, and ours from both pressure and optical informatiuons. The inset is a spectrum involved.

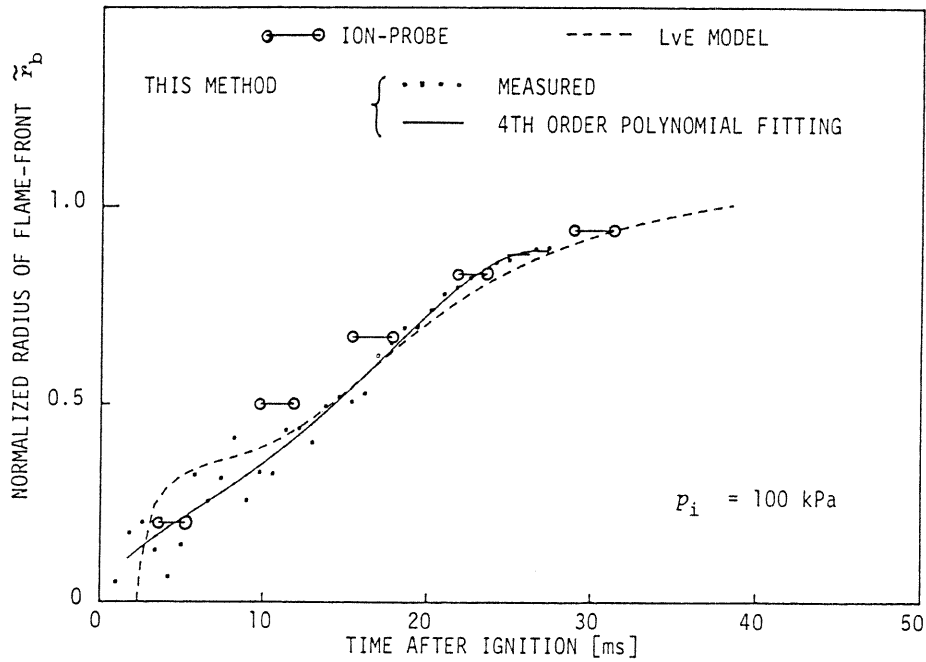


Fig.12 Progress of flame-front radii for $p_i=100$ kPa.

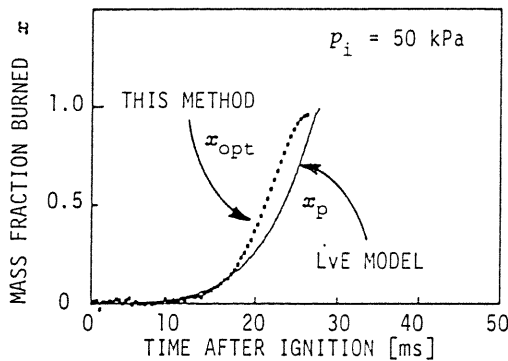


Fig.13 Mass fraction burned for $p_i=50$ kPa.

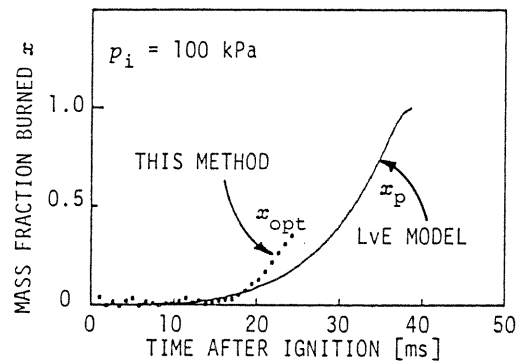


Fig.14 Mass fraction burned for $p_i=100$ kPa.

The mass fraction burned, x , was calculated from these data with using both our method of eq.(11) and LVE model of eq.(12), as shown in Fig.13 and 14. Two results coincide in the initial stages but differ in the last stage where accuracies of our method deteriorates due to the pressure-broadening of the absorption line of methane beyond the spectral coverage of Pb-TDL employed here.

CONCLUSIONS

A new method with a tunable lead-salt diode laser was applied to continuously measure the mass fraction burned of stoichiometric methane-air mixture held in a spherical vessel. The method of involving a spectral information made it possible to measure abundance of unburned methane suffered from the increasing pressure broadening. It was demonstrated also that this method is effective at the initial stage of a combustion in a spherical vessel exploiting a

noncontacting measurement capability which is to promise a very local sounding of a combustion.

Further improvements is however necessary to extend the width of spectral scanning of the diode laser in order for this method be component for wider aspects of combustion analysis.

Acknowledgements

The authors are indebted to energetic participations into the experiments of K. Awamoto and T. Okada and other students of Okayama University. The PbSnTe diode laser and infrared detectors were supplied by Dr. K. Shinohara of Fujitsu Laboratories Ltd. The authors would express their thanks to these people for their cooperations.

This work was supported by a Grant in Aid for Special Project Research from the Ministry of Education, Science and Culture of Japan.

NOMENCLATURE

a = inner radius of spherical vessel
 I = apparent line intensity
 $I_i = I$ at the ignition
 $\tilde{I} = I$ normalized by I_i
 n = molecular density of methane
 p = pressure
 p_e = pressure at the final stage
 p_i = pressure at the ignition
 $\tilde{p} = p$ normalized by p_i
 r_b = flame radius
 x = mass fraction burned
 $x_{opt} = x$ obtained by optical and pressure data
 $x_p = x$ obtained only with pressure, p
 W_I = incidence power of laser beam
 W_T = transmitted power of laser beam
 α = half width at half maximum of Lorentzian line profile
 $\alpha_i = \alpha$ at the ignition
 λ = ratio of specific heat with constant pressure to that of constant volume
 ν = wavenumber of the infrared probe laser light
 θ_i = temperature of the gas before the ignition
 θ_u = temperature of unburned gas
 τ = optical thickness of methane.

Subscripts

i = initial value just at the ignition
 opt = calculated with the optical data, \tilde{I} , and with the pressure, \tilde{p}
 p = calculated only from the pressure, \tilde{p}

REFERENCES

1. Tabaczynski, R.J., Trinker, F.H. and Shannon, B.A.S., Further Refinement and Validation of a Turbulent Flame Propagation Model for Spark-Ignition Engines, *Combustion and Flame*, Vol.39, pp.111-121, 1980.
2. Takeno, T. and Iijima, T., Theoretical study of Nonsteady Flame Propagation in Closed Vessels, *Progress in Astronautics and Aeronautics*, Vol.77, *Combustion in Reactive Systems*, Edited by Bowen, J.R., Manson, N., Oppenheim, A.K. and Soloukhin, American Institute of Aeronautics and Astronautics, pp.578-595.
3. Metghalchi, M. and Keck, J.C., Laminar Burning Velocity of Propane-Air Mixture at High Temperature and Pressure, *Combustion and Flame*, Vol.38, pp.143-154, 1980.
4. Dyer, T.M., Characterization of One and Two-Dimensional Homogeneous Combustion Phenomena in Constant Volume Bomb, *SAE Trans.*, Vol.88, Sect.2, pp.1196-1216, Paper No.79035, 1979.
5. Kalghatgi, G.T. and Swords, M.D., Flame-Speed Measurements in an Internal Combustion Engine, *Combustion and Flame*, Vol.49, pp.163-169, 1983.
6. Preier, H., Recent Advances in Lead-Chalcogenide Diode Lasers, *Appl. Phys.* Vol.20, pp.189-206, 1976.
7. Koga, R., Kosaka, M., and Sano, H., Field Methane Tracking with a portable and real-time open-gas monitor based on a cw-driven Pb-salt diode laser, *Optics and Laser Technology*, to be published in Vol.17, 1985.
8. Nagase, S., Koga, R., Kosaka, M., and Sano, H., A Method to Measure the Thermal Time Constant of a Diode Laser., *Transac., Inst. Electron. Communication Eng.*, Vol.63-C, pp.317-318, 1980.
9. McCartney, E.J., "Absorption and Emission by Atmospheric gases" John Wiley & Sons, p.217, 1983
10. Lewis, B. and von Elbe, G., "Combustion, Flames and Explosions of Gases," Academic Press, pp.367-381, 1961.
11. Sano, H., Koga, R., Kosaka, M., and Shinohara, K., High sensitivity Short-Path Monitoring of Trace Gases Employing PbSnTe Tunable Diode Laser, *Japan. J. Appl. Phys.*, Vol.20, pp.2145-2153, 1981.